WATER RESOURCES RESEARCH, VOL. 37, NO. 5, PAGES 1277–1290, MAY 2001

Space-time modeling of water table depth using a regionalized time series model and the Kalman filter

Marc F. P. Bierkens, M. Knotters, and T. Hoogland
Alterra, Wageningen University and Research Centre, Wageningen, Netherlands

Abstract. The spatiotemporal variation of shallow water table depth is modeled with a regionalized version of an autoregressive exogenous (ARX) time series model. The ARX model relates the temporal variation of the water table depth at a single location to a time series of precipitation surplus. The ARX model is calibrated first at locations where time series of water table depth are available. ARX parameters at nonvisited locations are estimated through geostatistical interpolation using auxiliary information, resulting in a regionalized ARX model or RARX model. The parameters of the geostatistical model are estimated by embedding the RARX model in a space-time Kalman filter and minimization of a maximum likelihood criterion built from the filter innovations. The resulting state estimator can be used for optimal space-time prediction of water table depth, network optimization, and space-time conditional simulation.

1. Introduction

Water table depth is an important factor in managing lowland rural areas. For instance, during the growing season shallow water tables can be an important source of water for crops. In addition, the water table depth has a large impact on soil temperature and soil trafficability at the beginning of the growing season. Furthermore, many nature areas such as wetlands rely on a very specific regime of the water table depth, as well as on the associated groundwater quality. Also, the leaching of nutrients and pesticides is largely influenced by the water table depth and its variation during the year. These examples show that knowledge of the variation of the water table depth in both space and time is important for successful land use planning, engineering, and operational management in rural areas.

As it is impossible to observe the water table depth everywhere all the time, an interpolation method is required to obtain a complete spatiotemporal picture. Obviously, the most natural candidate to perform this interpolation is a numerical groundwater flow model that solves the partial differential equation of hydraulic head in space and time. The problem with this approach is that in many lowland areas the water table depth is not controlled by transmissivity and groundwater recharge alone. Instead, small-scale variations are present that depend on local topography, soil type, and a dense drainage network. The amount of data and modeling detail that is needed to include these factors in a groundwater flow model is enormous. Therefore, although much more costly, not much can be gained by applying such models when compared to more empirical interpolations methods. This is particularly the case if the goal is space-time interpolation (e.g., inventory and monitoring), instead of extrapolation or scenario analysis.

Statistical methods for space-time prediction thus are a valid alternative if the primary goal is space-time interpolation for inventory and monitoring purposes. All statistical space-time prediction methods in some way parameterize the spatiotemporal stochastic function $Z(\mathbf{x}, t)$. However, the form of this parameterization can be very different between methods. Traditionally, there have been two different approaches: (1) methods starting from a geostatistical methodology, applying space-time kriging or cokriging [*Rouhani and Hall*, 1989; *Bogaert*, 1996; *Heuvelink et al.*, 1997], and (2) methods based on multivariate time series analysis, where multiple time series are analyzed that are correlated in space [*Bennet*, 1979; *Pfeifer and Deutsch*, 1980; *Haslett and Raftery*, 1989]. During recent years many methods have been proposed that are in some way combinations of both approaches [*Guttorp et al.*, 1994; *Huang and Cressie*, 1996; *Wikle and Cressie*, 1999; *Angulo et al.*, 1998]. *Kyriakides and Journel* [1999] provide a recent review of statistical space-time modeling.

One type of combination approach is the use of time series models with regionalized parameters [*Guttorp et al.*, 1994; *Hutchinson*, 1995; *Guenni et al.*, 1996; *Van Geer and Zuur*, 1997; *Knotters and Bierkens*, 2001]. Here the temporal variation is modeled with a time series model (usually discrete in time), whose parameters are a continuous function of location and whose noise components are spatially colored. These approaches are typically useful if data are dense in time and sparse in space, for example, time series of water table depth at a limited number of locations.

In this paper a method is introduced that belongs to the latter category of approaches to statistical space-time modeling. The temporal variation of water table depth is modeled with a discrete-time autoregressive exogenous variable model or ARX model [*Hipel and McLeod*, 1994], where precipitation surplus is used as an exogenous variable. The ARX model is calibrated at locations where time series of water table depth are available. ARX parameters at nonvisited locations are estimated through geostatistical interpolation using auxiliary information, such as digital elevation models and catchment boundaries. This results in a regionalized ARX (RARX) model. The parameters of the geostatistical model (e.g., the semivariogram) are estimated by embedding the RARX model in a space-time Kalman filter and minimization of a maximum likelihood criterion built from the filter innovations. The resulting state estimator can be used for optimal space-time prediction of water table depth, network optimization, and

Paper number 2000WR900353.
0043-1397/01/2000WR900353$09.00

stochastic space-time conditional simulation. Compared to similar approaches to space-time Kalman filtering [*Wikle and Cressie*, 1999] or smoothing [*Angulo et al.*, 1998], the method introduced here differs in two distinct ways. First, auxiliary information is used in a geostatistical framework to spatially interpolate the parameters of the time series model. Second, apart from space-time prediction, the Kalman filter is also used to estimate the parameters of the geostatistical models. The first property is particularly useful if the number of time series is very limited, such that interpolation without auxiliary information is very inaccurate.

The remainder of this paper is organized as follows. A regionalized ARX (RARX) model [*Knotters and Bierkens*, 2001] for water table depth is introduced first. After that, we describe how the RARX model is calibrated to observed time series and incidental observations. Next, it is explained how the calibrated RARX model is used for space-time prediction and space-time conditional simulation. Thereafter a case study is presented where the methods are applied and validated. The paper ends with some concluding remarks and discussion.

2. A Regionalized ARX Model for Water Table Depth

In this section we develop the spatiotemporal model of water table depth.

2.1. ARX Model for Water Table Depth

The depth of shallow water tables at discrete time steps $t = 0, 1, 2 \ldots$ is modeled using a first-order autoregressive exogenous variable model (ARX(1, 0)):

$$H_t - c = a\{H_{t-1} - c\} + bP_t + \varepsilon_t, \tag{1}$$

where H_t is the water table depth $[L]$ (height of the phreatic surface with respect to surface elevation). P_t is the average precipitation surplus between $t - 1$ and t $[L\ T^{-1}]$, which is calculated as the average precipitation minus the average potential evapotranspiration, observed at a nearby meteostation. Parameters a and b determine the dynamic response of the water table, and c is a parameter determining the average water table depth in case $P_t = 0$. The variable ε_t is a discrete white noise process with the following properties:

$$E[\varepsilon_t] = 0$$
$$E[\varepsilon_t\varepsilon_s] = \begin{cases} \sigma^2 & t = s \\ 0 & t \neq s. \end{cases} \tag{2}$$

The choice of (1) is not based on some model selection criterion (such as Akaike's information criterion), but it is chosen because it can be interpreted in physical terms. In fact, if the water balance of the combined soil-water and shallow groundwater system is analyzed, assuming no surface runoff and a linear relation between water table depth and drainage from the groundwater zone to the surface water, the water table fluctuation for discrete time steps is described with an equation exactly like (1) [*Knotters and Bierkens*, 2001]. Other exogenous variables such as groundwater withdrawal rates and varying surface water levels can be added straightforwardly.

2.2. Regionalized ARX Model

A regionalized ARX (RARX) model [*Knotters and Bierkens*, 2001] describing the spatiotemporal variation of water table depth is built by making the ARX parameters location dependent:

$$H_t(\mathbf{x}) - c(\mathbf{x}) = a(\mathbf{x})\{H_{t-1}(\mathbf{x}) - c(\mathbf{x})\} + b(\mathbf{x})P_t + \varepsilon_t(\mathbf{x}), \tag{3}$$

where $\mathbf{x}$ is the vector with spatial coordinates: $\mathbf{x}^T = (x, y)$. Note that this model describes the water table depth discretely in time and continuously in space. Also, note that the precipitation surplus is assumed to be global, i.e., space invariant. This assumption is reasonable if the model is applied in small areas such as used in the case study hereafter. The noise process is now assumed to be discrete and white in time but continuous and colored in space with an isotropic exponential spatial covariance:

$$E[\varepsilon_t(\mathbf{x})] = 0$$
$$E[\varepsilon_t(\mathbf{x}_1)\varepsilon_s(\mathbf{x}_2)] = \begin{cases} \sigma(\mathbf{x}_1)\sigma(\mathbf{x}_2)\exp\left[-\dfrac{|\mathbf{x}_2 - \mathbf{x}_1|}{I}\right] & t = s \\ 0 & t \neq s, \end{cases} \tag{4}$$

where I is the spatial integral scale of the additive noise process. Note that this model allows for the noise to be spatially heteroscedastic, that is, to have different variances at different locations. The noise process is expected to be spatially dependent for two reasons. First, if during some extreme event the water table depth at some location is underestimated by the model, it is likely to be underestimated at a nearby location as well. Second, the RARX model omits spatial interaction through the system dynamics; that is, $H_t(\mathbf{x})$ only depends on the past at the same location $H_{t-1}(\mathbf{x})$ but not on another location nearby (e.g., $H_{t-1}(\mathbf{x} + \Delta\mathbf{x})$), as would a numerical groundwater flow model. This omitted spatial interaction will manifest itself as colored noise.

2.3. Regionalization Functions

To apply the model at a set of nonvisited locations, the RARX parameters $a(\mathbf{x})$, $b(\mathbf{x})$, $c(\mathbf{x})$, and $\sigma(\mathbf{x})$ must be known at these locations. In practice, these parameters are only known at the locations where time series of water table depth have been recorded, where they can be obtained through calibration of the ARX model (1) (see *Bierkens et al.* [1999] for an example). Consequently, the RARX parameters must somehow be estimated at the unvisited locations, using the values of these parameters found at the locations with time series. However, these are usually few, so it would be useful to be able to include exhaustive auxiliary information in the estimator. For instance, elevations from a digital elevation model (DEM) may be correlated with some of the RARX parameters and therefore may be used. Likewise, soil maps or a map with (sub) catchment boundaries may be useful auxiliary information.

To include all this in estimating the RARX parameters, we propose a general estimator which we will denote as a "regionalization function." For instance, for the parameter a at a unvisited location we have

$$\hat{a}(\mathbf{x}) = r_a(\mathbf{x};\ a(\mathbf{x}_i),\ i = 1, \ldots, n;\ s(\mathbf{x});\ \boldsymbol{\theta}_a), \tag{5}$$

where

- $\hat{a}(\mathbf{x})$ estimate of $a(\mathbf{x})$;
- $r_a(\ )$ regionalization function;
- $a(\mathbf{x}_i)$ known values of a at n locations with time series of observed water table depth located at $\mathbf{x}_i$, $i = 1, \ldots, n$;

$s(\mathbf{x})$ value of exhaustive auxiliary information at location $\mathbf{x}$; (For simplicity, it is implied here that only one auxiliary variable is used for one RARX parameter and that this variable is exhaustively sampled. However, the approach can easily be generalized to include nonexhaustive and multivariate auxiliary information.)

$\boldsymbol{\theta}_a$ vector of parameters determining the shape of $r_a(\ )$.

Similar functions are defined for $b(\mathbf{x})$, $c(\mathbf{x})$, and $\sigma(\mathbf{x})$. Regionalization functions can be of any shape and form, for example, stratification, Thiessen polygons, inverse distance, splines, regression, and kriging. For instance, if $a(\mathbf{x})$ is interpolated from the locations with time series using kriging with an external drift [*Goovaerts*, 1997], $r_a(\ )$ would have the following form:

$$r_a(\mathbf{x}; \ldots) = \sum_{i=1}^{n} \lambda_i(\boldsymbol{\theta}_a) a(\mathbf{x}_i), \tag{6}$$

with weights such that

$$\beta(s(\mathbf{x})) = \sum_{i=1}^{n} \lambda_i(\boldsymbol{\theta}_a) \beta(s(\mathbf{x}_i)),$$

where $\beta(\ )$ is a drift function depending on the auxiliary variable $s(\mathbf{x})$, $\lambda_i(\ )$ represents kriging weights depending on the parameter vector $\boldsymbol{\theta}_a$, and $\boldsymbol{\theta}_a$ is a set of parameters determining the geostatistical model, in this case the parameters of the semivariogram of residuals.

Another example would be the stratification of the spatial domain in m strata, for instance, based on the polygons of a soil map. In that case, $r_a(\ )$ would produce a fixed value for each stratum, the auxiliary variable $s(\mathbf{x})$ would be the stratum number $(1, \ldots, m)$, and $\boldsymbol{\theta}_a$ would be a vector of m stratum means. We stress that in this modeling framework the regionalization functions are viewed as purely deterministic, that is, as a way to reduce the large RARX parameter space occupied by $a(\mathbf{x})$, $b(\mathbf{x})$, $c(\mathbf{x})$, and $\sigma(\mathbf{x})$ to a few spatial functions of predefined form and a limited set of parameters.

3. Calibration of the RARX Model

To apply the RARX model, the parameters $\boldsymbol{\theta}$ of the regionalization functions must be found so that the RARX parameters at unvisited locations can be estimated through (5). One way to do this is by calibration; that is, the RARX model is used to predict time series at locations where observations of the water table depth are available. The most appropriate values of the $\boldsymbol{\theta}$ (e.g., semivariogram parameters) are obtained by minimizing the differences between the water table depths calculated with the RARX model and the observations. In this section such a procedure is given. The procedure depends on a number of additional requirements, each of which is described in sections 3.1–3.4: a state-space formulation, the Kalman filter, a maximum likelihood estimator, and possibly additional sampling.

3.1. State-Space Formulation

To calibrate the RARX model, preferably all available observations of water table depth are used, especially if observations are rare. State-space prediction methods such as the Kalman filter [*Schweppe*, 1973] provide a framework for predicting variables at nonobserved locations and nonobserved time steps using observations that are irregularly distributed both in space and time. Also, data of different quality can be used, because observation errors can be taken into account. To be able to apply the Kalman filter to the RARX model, it must first be written in state-space formulation.

Suppose that we have a set of N locations where the water table depth is to be predicted for discrete time steps $t = 0, 1, 2, \ldots, K$. The N locations also include all the locations where at some of the time steps an observation of the water table depth is available. If we set up the RARX model (equation (3)) for the N locations using the estimated values of the RARX parameters, the RARX model can be written in state-space formulation as follows:

$$\begin{pmatrix} H_t(\mathbf{x}_1) \\ H_t(\mathbf{x}_2) \\ \vdots \\ H_t(\mathbf{x}_N) \end{pmatrix} = \begin{pmatrix} \hat{a}(\mathbf{x}_1) & 0 & \cdots & 0 \\ 0 & \hat{a}(\mathbf{x}_2) & \ddots & \vdots \\ \vdots & \ddots & \ddots & 0 \\ 0 & \cdots & 0 & \hat{a}(\mathbf{x}_N) \end{pmatrix} \begin{pmatrix} H_{t-1}(\mathbf{x}_1) \\ H_{t-1}(\mathbf{x}_2) \\ \vdots \\ H_{t-1}(\mathbf{x}_N) \end{pmatrix}$$
$$+ \begin{pmatrix} 1 - \hat{a}(\mathbf{x}_1) & 0 & \cdots & 0 & \hat{b}(\mathbf{x}_1) \\ 0 & 1 - \hat{a}(\mathbf{x}_2) & \ddots & & \hat{b}(\mathbf{x}_2) \\ \vdots & \ddots & \ddots & 0 & \vdots \\ 0 & \cdots & 0 & 1 - \hat{a}(\mathbf{x}_N) & \hat{b}(\mathbf{x}_N) \end{pmatrix}$$
$$\cdot \begin{pmatrix} \hat{c}(\mathbf{x}_1) \\ \hat{c}(\mathbf{x}_2) \\ \vdots \\ \hat{c}(\mathbf{x}_N) \\ P_t \end{pmatrix} + \begin{pmatrix} \varepsilon_t(\mathbf{x}_1) \\ \varepsilon_t(\mathbf{x}_2) \\ \vdots \\ \varepsilon_t(\mathbf{x}_N) \end{pmatrix}. \tag{7}$$

The circumflexes are used to denote that the ARX parameters are estimated using regionalization functions. This way of writing the RARX model is quite convenient. If another global exogenous variable is added, for instance, a groundwater withdrawal Q_t, this only entails adding a new column to the $N \times (N + 1)$ matrix on the right, for instance, with the parameters $\hat{d}(\mathbf{x}_1), \ldots, \hat{d}(\mathbf{x}_N)$ and adding the observed Q_t, as an element below P_t. Also, because they are part of the input vector, the average water table depths $\hat{c}(\mathbf{x}_i)$ can be easily made to vary with time, for instance, by linking them to varying surface water levels [*Knotters and Bierkens*, 2000].

Using $\mathbf{h}_t$ for the $N \times 1$ vector on the left side (state vector), $\mathbf{A}$ for the $N \times N$ matrix on the right-hand side (system matrix), $\mathbf{B}$ for the $N \times (N + 1)$ matrix on the right-hand side (input matrix), $\mathbf{u}_t$ for the $(N + 1) \times 1$ input vector, and $\mathbf{e}_t$ for the $N \times 1$ vector with additive noise, (7) is written as

$$\mathbf{h}_t = \mathbf{A}(\boldsymbol{\theta}_a)\mathbf{h}_{t-1} + \mathbf{B}(\boldsymbol{\theta}_a, \boldsymbol{\theta}_b)\mathbf{u}_t(\boldsymbol{\theta}_c) + \mathbf{e}_t. \tag{8}$$

Equation (8) is called the state equation. Note that we have added the vectors $\boldsymbol{\theta}$ to the equation to denote that the elements in the matrices depend on the parameters used in the regionalization functions; that is, in case of a geostatistical interpolation of the RARX parameters they depend on the parameters of the semivariograms used.

On the basis of (4) the noise vector has the following properties:

$$E[\mathbf{e}_t \mathbf{e}_s^{\mathrm{T}}] = \begin{cases} \mathbf{Q}(\boldsymbol{\theta}_\sigma, I) & t = s \\ \mathbf{0} & t \neq s, \end{cases} \tag{9}$$

where $\mathbf{Q}$ is the $N \times N$ noise covariance matrix which is also a function of the parameters of the regionalization function and a function of a global parameter, the integral scale I. The elements $[Q_{ij}]$ of the noise covariance matrix are then given by

$$[Q_{ij}] = \hat{\sigma}(\mathbf{x}_i; \boldsymbol{\theta}_\sigma)\hat{\sigma}(\mathbf{x}_j; \boldsymbol{\theta}_\sigma) \exp(-|\mathbf{x}_j - \mathbf{x}_i|/I). \quad (10)$$

3.2. Kalman Filter

The (linear) Kalman filter is based on the state equation (8) and an equation linking observations to the state. This equation, called the measurement equation, is given by

$$\mathbf{y}_t = \mathbf{C}_t\mathbf{h}_t + \mathbf{v}_t. \quad (11)$$

If at time step t $M_{\mathbf{y},t}$ observations are taken, then $\mathbf{y}_t$ is a $M_{\mathbf{y},t} \times 1$ vector with observations and $\mathbf{C}_t$ is a $M_{\mathbf{y},t} \times N$ matrix called the measurement matrix. If all locations at which at some time an observation is taken are included in the state, the matrix $\mathbf{C}_t$ has the following form. For row $i = 1, \ldots, M_{\mathbf{y},t}$, if element i of $\mathbf{y}_t$ is an observation of the state variable located in row j of $\mathbf{h}_t$, then element (i, j) of $\mathbf{C}_t$ is set to "1"; all other elements of row i of $\mathbf{C}_t$ are set to "0." The vector $\mathbf{v}_t$ is a noise vector representing the measurement error with the following properties:

$$E[\mathbf{v}_t] = \mathbf{0}$$
$$E[\mathbf{v}_t\mathbf{v}_s^T] = \begin{cases} \mathbf{R}_t & t = s \\ \mathbf{0} & t \neq s, \end{cases} \quad (12)$$

where $\mathbf{0}$ is the null vector or null matrix and $\mathbf{R}$ is a covariance matrix of observation errors. Usually, it is assumed that the observation errors are independent, which means that $\mathbf{R}_t$ is a diagonal matrix with the variances of the observation errors on the diagonal. The observation errors are independent of the system noise:

$$E[\mathbf{v}_t\mathbf{e}_s^T] = \mathbf{0} \qquad \forall\, t, s. \quad (13)$$

With the state equation (8), the measurement equation (11), and the properties of the error processes as denoted in (9), (10), (12), and (13), the Kalman filter can be applied to obtain optimal predictions of the state vector $\mathbf{h}_t$. The Kalman filter algorithm is well known and is not repeated here. We refer to *Van Geer et al.* [1991] for an example of a complete description.

3.3. Maximum Likelihood Estimation

As explained in section 3.1, the matrices $\mathbf{A}$ and $\mathbf{B}$ and the vector $\mathbf{u}$ depend on the regionalization parameters $\boldsymbol{\theta}_a$, $\boldsymbol{\theta}_b$, and $\boldsymbol{\theta}_c$ and the covariance matrix $\mathbf{Q}$ on $\boldsymbol{\theta}_\sigma$ and the integral scale I. Therefore, through the state equation the differences between the Kalman filter predictions and the observations also depend on these parameters. Consequently, one way of estimating the set of parameters $\boldsymbol{\Theta}^T = (\boldsymbol{\theta}_a^T, \boldsymbol{\theta}_b^T, \boldsymbol{\theta}_c^T, \boldsymbol{\theta}_\sigma^T, I)$ is by running the Kalman filter and minimizing the Kalman filter prediction errors. Under the assumption that both the system noise $\mathbf{e}_t$ and the observation errors $\mathbf{v}_t$ are Gaussian distributed, a maximum likelihood (ML) estimate of the parameters $\boldsymbol{\Theta}$ is obtained by minimizing the following criterion [*Schweppe*, 1973]:

$$J(L; \boldsymbol{\Theta}) = LM_{\mathbf{y}} \ln(2\pi) + \sum_{l=1}^{L} \ln(|\mathbf{Z}_l(\boldsymbol{\Theta})|) + \sum_{l=1}^{L} \mathbf{n}_l^T(\boldsymbol{\Theta})\mathbf{Z}_l^{-1}(\boldsymbol{\Theta})\mathbf{n}_l(\boldsymbol{\Theta}), \quad (14)$$

where J is the log likelihood and $\mathbf{n}_l$ is the vector of differences between the observations $\mathbf{y}_l$ and the time update $\bar{\mathbf{h}}_l$ at time step l: $\mathbf{n}_l = \mathbf{y}_l - \mathbf{C}_l\bar{\mathbf{h}}_l$. The time update $\bar{\mathbf{h}}_l$ is the Kalman filter prediction using all observations up to and including time step $l - 1$. $\mathbf{Z}_l$ is the covariance matrix of $\mathbf{n}_l$: $E[\mathbf{n}_l\mathbf{n}_l^T]$. L is the number of times at which observations have been taken and $M_{\mathbf{y}}$ is the average number of observations per observation time.

Summarizing, if the regionalization of the ARX parameters is performed by geostatistical interpolation, the calibration of the RARX model using the Kalman filter and the ML criterion (14) is performed by the following procedure.

1. Calibrate the ARX model of (1) at each location where long time series of water table depth are available (these locations are denoted "time series locations"). This yields the RARX parameters $a(\mathbf{x})$, $b(\mathbf{x})$, $c(\mathbf{x})$, and $\sigma(\mathbf{x})$ at the time series locations. We refer to *Bierkens et al.* [1999] for a procedure to calibrate the ARX model (1) to irregularly observed time series of water table depth.
2. Choose the regionalization function (i.e., the type of kriging approach) and the initial set of regionalization parameters $\boldsymbol{\Theta}$ (i.e., the parameters of the semivariograms).
3. Regionalize (e.g., interpolation by ordinary kriging) to obtain the RARX parameters at all locations of the state: $\hat{a}(\mathbf{x})$, $\hat{b}(\mathbf{x})$, $\hat{c}(\mathbf{x})$, and $\hat{\sigma}(\mathbf{x})$.
4. Run the Kalman filter with these parameters and evaluate ML criterion (14).
5. Adjust the regionalization parameters $\boldsymbol{\Theta}$ based on the value of the ML criterion and go to step 3. Steps 3–5 are repeated until convergence.

To minimize (14), we used the downhill simplex method [*Press et al.*, 1986] which does not require the derivatives of $J(L; \boldsymbol{\Theta})$. As explained in Appendix A, during calibration the size of the state vector is not larger than the number of locations where at some time observations are taken. For most practical problems this will not lead to large storage requirements or excessive computation times.

3.4. Calibration Locations

If a calibration scheme is used as described in section 3.3 and the regionalization functions involve exact interpolation methods such as kriging, apart from sufficiently long time series of water table depth, additional incidental observations of water table depth are required. Remember that an ARX model is calibrated at each time series location first (step 1 of section 3.3) yielding the RARX parameters at these locations. After that, the RARX parameters at the time series locations are geostatistically interpolated to the rest of the state locations (step 3 of section 3.3). If a criterion like (14) is used to estimate the parameters $\boldsymbol{\theta}_a$, $\boldsymbol{\theta}_a$, $\boldsymbol{\theta}_c$, and $\boldsymbol{\theta}_\sigma$, it must of course depend on these parameters. For a regionalization function that is an exact interpolator (like kriging) this is only the case if, apart from observations at the locations where the RARX parameters are known (the time series locations), additional observations at other state locations are collected, preferably at varying distance from the time series locations (i.e., to check whether the interpolation is successful). At these additional locations, which we will denote as "calibration locations," it is not necessary to have long time series. Observations at a limited number of well-chosen time steps are sufficient, while it is probably better to strive for a high spatial coverage than for a high frequency (i.e., to have more calibration locations and less observations per calibration location). Note that the "calibration" in calibration locations refers to calibrating the RARX model, i.e., finding the parameters $\boldsymbol{\Theta}^T = (\boldsymbol{\theta}_a^T, \boldsymbol{\theta}_b^T, \boldsymbol{\theta}_c^T, \boldsymbol{\theta}_\sigma^T, I)$, and not to step 1 of section 3.3. If calibration locations are not present, additional sampling may be required. Alternatively,

suboptimal solutions can be used, such as cross validation or jackknifing or choosing a regionalization function that is not an exact interpolator, such as a regression surface.

4. Space-Time Prediction

Once the parameters Θ of the RARX model have been estimated using the Kalman filter for a limited state (time series locations and calibration locations, see Appendix A), the Kalman filter can be used for space-time prediction of the complete state. Thus the state vector is extended to include not only the locations with observations but all locations where the water table depth is to be predicted. Once the state has been determined, the space-time prediction proceeds as follows: (1) Using the calibrated parameter values $\hat{\Theta}$, regionalize/interpolate to obtain the RARX parameters $\hat{a}(\mathbf{x})$, $\hat{b}(\mathbf{x})$, $\hat{c}(\mathbf{x})$, and $\hat{\sigma}(\mathbf{x})$ at all locations of the state. (2) With the RARX parameters and the estimated integral scale $\hat{I}$ of the system noise covariance matrix (see (10)), run the Kalman filter to obtain optimal predictions of $\mathbf{h}_t(\mathbf{x})$ for $t = 0, 1, \ldots, K$. The optimal prediction at time step t is given by the measurement update $\hat{\mathbf{h}}_t$, which is the Kalman filter prediction using all observations up to and including time step t.

If the system noise and the observation errors are Gaussian, the measurement update is the conditional expected value of $\mathbf{h}_t$ given all observations up to and including time step t: $\hat{\mathbf{h}}_t = E[\mathbf{h}_t|\mathbf{y}_t^T, \mathbf{y}_{t-1}^T, \ldots, \mathbf{y}_0^T]$. The associated covariance matrix of the prediction error $\mathbf{\Sigma}_{t|t} = E\{[\hat{\mathbf{h}}_t(\mathbf{x}) - \mathbf{h}_t][\hat{\mathbf{h}}_t(\mathbf{x}) - \mathbf{h}_t]^T\}$ is the conditional covariance. In Appendix A it is explained that if we are only interested in the prediction variances, i.e., the diagonal of $\mathbf{\Sigma}_{t|t}$, a location by location prediction method can be applied that enables the use of large states (thousands of locations) without storage problems and large computation times.

5. Space-Time Conditional Simulation

Under the assumption that $\mathbf{h}_t$ is multivariate Gaussian distributed, the full conditional multivariate distribution of $\mathbf{h}_t$ (given all observations up to and including time step t) is fully defined by $\hat{\mathbf{h}}_t$ and $\mathbf{\Sigma}_{t|t}$. Therefore, in theory it is possible to calculate the probability distribution of any model outcome that has the water table depth as input. However, if this model is nonlinear and its outcome depends on the values of the water table depth at multiple locations and multiple time steps, deriving the distribution of model outcomes is very cumbersome, and a Monte Carlo approach is preferred. This would involve the simulation of realizations of temporally and spatially correlated random variables (i.e., realizations from a space-time random field conditional to the observations). The Kalman filter can be used for this purpose.

To simulate at a finite number of locations a realization of the space-time stochastic process $\{H_t(\mathbf{x}), t = 0, 1, \ldots, K\}$ that for each time step t is conditional to all observations taken up to and including time step t (for each t conditional to $\{\mathbf{y}_t^T, \mathbf{y}_{t-1}^T, \ldots, \mathbf{y}_0^T\}$), the Kalman filter can be used in the following way: (1) Using the calibrated parameter values $\hat{\Theta}$, regionalize/interpolate to obtain the RARX parameters $\hat{a}(\mathbf{x})$, $\hat{b}(\mathbf{x})$, $\hat{c}(\mathbf{x})$, and $\hat{\sigma}(\mathbf{x})$ at all locations of the state. (2) With the RARX parameters and the estimated integral scale $\hat{I}$ of the system noise covariance matrix, run the Kalman filter for all state locations for $t = 0, 1, \ldots, K$, where the usual equation for the time update is replaced with the following stochastic equation:

$$\bar{\mathbf{h}}_t = \mathbf{A}\hat{\mathbf{h}}_{t-1} + \mathbf{B}\mathbf{u}_t + \mathbf{L}\mathbf{g}_t, \tag{15}$$

where $\mathbf{g}_t$ is a vector of simulated independent standard Gaussian deviates and $\mathbf{L}$ is the lower triangular of the Cholesky decomposition of the covariance matrix $\mathbf{Q}$.

This procedure is known as the "ensemble Kalman filter" [*Evensen and Van Leeuwen*, 1995] and was originally designed to solve nonlinear filter problems without the need for linearization. In Appendix A it is explained how this algorithm can be applied to large states without storage problems and excessive computation times. We stress that the realizations so obtained are not conditional to all observation taken between $t = 0, 1, \ldots, K$. For instance, the partial realization $H_t(\mathbf{x})$ is only conditional on observations $\{\mathbf{y}_t^T, \mathbf{y}_{t-1}^T, \ldots, \mathbf{y}_0^T\}$. For $H_t(\mathbf{x})$ to be conditional on all observations $\{\mathbf{y}_K^T, \mathbf{y}_{K-1}^T, \ldots, \mathbf{y}_t^T, \ldots, \mathbf{y}_0^T\}$, a Kalman smoother must be implemented. This, however, is somewhat less straightforward than application of the Kalman filter, especially when used for stochastic simulation, while the reduction of uncertainty is not always significant.

6. Case Study

6.1. Description of the Study Area

Figure 1 shows the outline of the study area (1375 ha) and its position in the Netherlands. Three types of locations are shown: 14 locations where piezometers have been present for a number of years and time series of water table depth are recorded (time series locations), 10 calibration locations, and 20 locations used only for validation. At the calibration locations and validation locations the water table depth has been measured occasionally (25 observations divided over five periods throughout 1997 and 1998). At all the locations with observations the surface elevation was determined by surveying.

Figure 1 also shows the borders between the catchments making up the area. Each catchment is, in fact, a "control unit" where the water boards try to maintain a prescribed surface water level, based on the relief, soil type, and land use within the catchment. Calibration locations and validation locations were selected by stratified random sampling with the catchments as strata (allocation number dependent on catchment size). Figure 2 shows a 25 × 25 m resolution DEM of the area, where surface elevations are denoted with respect to NAP (Dutch ordnance level). The southern part of the study area is bordered by a natural stream. The subsoil of lower areas (<8 m (NAP)) consist of wind-blown cover sands. In the lowest parts (<6 m (NAP)) these cover sands are overlain by clayey fluvial deposits and peat. The higher parts (>8 m (NAP)) in the north and northeast consist of boulder clays (glacial till) covered by thin layers of cover sands.

Precipitation surplus was calculated from daily observations of precipitation at a local weather station (approximately 5 km south of the study area) and potential evapotranspiration from a main weather station (40 km north of the study area). For potential evapotranspiration we used Makkink reference crop evapotranspiration [*De Bruin*, 1981; *Winter et al.*, 1995] which is routinely supplied by the Royal Netherlands Meteorological Institute and gives the potential evapotranspiration of a grass cover under optimal water supply. This yielded a time series of more than 32 years of daily precipitation surplus (January 1, 1966 to June 30, 1998). All calculations in the case study were performed with time steps of 1 day.

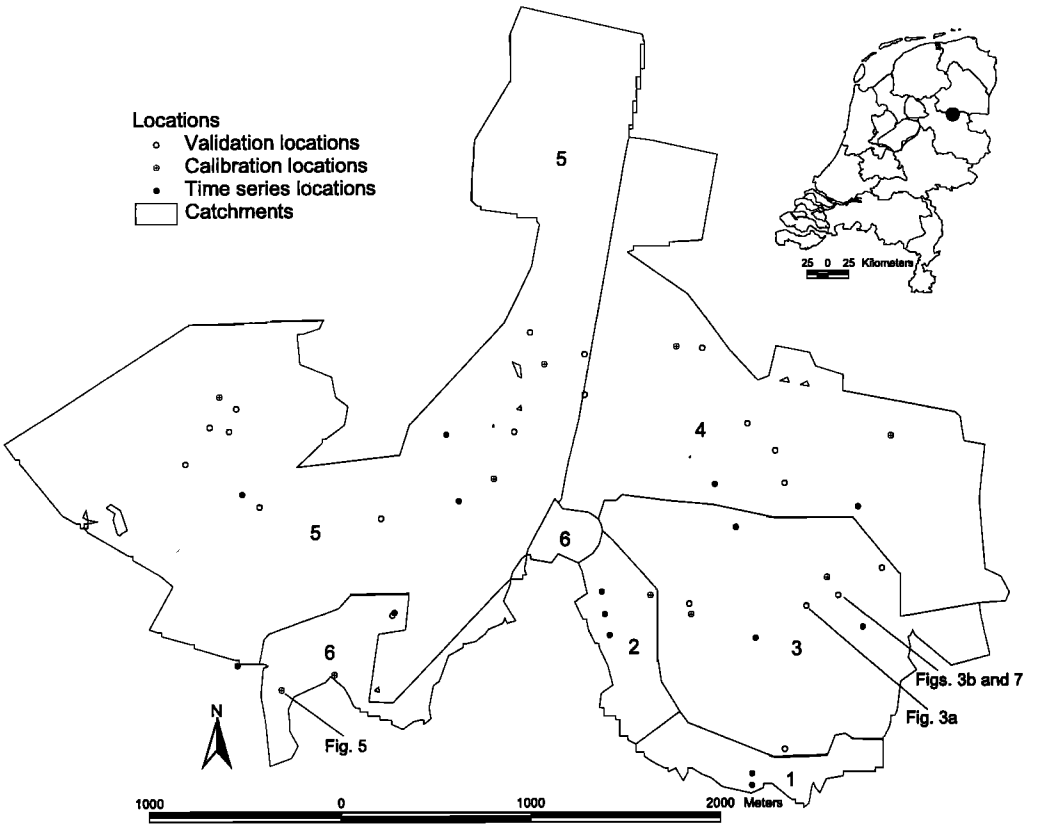

Figure 1. Map of the study area, its location, boundaries between catchments (surface water control units), and locations of observations of water table depth. Catchment 3 is "Paardelanden" where discharge has been observed.

6.2. Calibration and Validation

ARX models were first calibrated at the 14 time series locations. Next, using the ARX parameters and observations at the 14 time series locations and the observations at the 10 calibration locations, the RARX model was calibrated (see procedure section 3.3). At this calibration stage the state consisted of the 14 time series locations, the 10 calibration locations, and the 20 validation locations. The observations at the 20 validation locations were not used in the calibration procedure. However, after the RARX model was calibrated, the predicted water table depths at these locations were compared with the observations to validate the method. Observations were available for the period ranging from January 1, 1990, to June 30, 1998. During the calibration the Kalman filter was run for $K = 3834$ time steps, covering the period January 1, 1988, to June 30, 1998. So a 2-year "start up period" was used. The RARX model was calibrated using the following types of regionalization functions for the RARX parameters (see *Goovaerts* [1997] for elaborate descriptions of these methods): (1) ordinary kriging for all parameters (code OK); (2) simple kriging for all parameters (code SK); (3) simple kriging with known varying means for all parameters (code SKVk); (4) simple kriging with unknown varying means for all parameters (code SKVu); (5) kriging with external drift for all parameters, using the elevations of the digital elevation model as external drift variable (code KEDd); (6) a combination of methods 1–5 (code CM); and (7) kriging with external drift for all parameters, using the elevations obtained from surveying as external drift variable (code KEDs).

For method 3 for each stratum, which in this case is one of the catchments shown in Figure 1, a constant mean value is assumed and known. Method 4 is the same as SKVk, except that the stratum means are unknown and estimated implicitly. The combination method is constructed as follows: Methods 1–5 were used to obtain RARX parameters at the 14 time series locations by means of cross validation. For each parameter the method was chosen that yielded the closest estimate to the parameters obtained from calibrating the (one-dimensional) ARX model at the time series locations. This yielded the following combination: a (SKVk), b (SKVk), c (KEDd), and σ (OK). Method 7 was added for reference. Since exhaustive information about the surface elevation with the accuracy obtained from surveying is never present, this is not a method that could be used in practice.

For OK and SK the range parameters of the semivariograms are estimated using the Kalman filter and (14), for KEDd, KEDs, and SKVk the range parameters of the semivariograms of residuals are estimated, and for SKVu the semivariograms of residuals are assumed to be known, and the means of each stratum are estimated. Including the range parameter I used to calculate the covariance matrix (equations (9) and (10)), OK, SK, SKVk, KEDd, and KEDs required five parameters to be calibrated (ranges of parameters $a(\mathbf{x})$, $b(\mathbf{x})$, $c(\mathbf{x})$, and $\sigma(\mathbf{x})$ and the range parameter I), while the SKVu method required 25 parameters (six catchments, per catchment mean values of $a(\mathbf{x})$, $b(\mathbf{x})$, $c(\mathbf{x})$, and $\sigma(\mathbf{x})$, and the range parameter I).

The results of the calibration and validation procedure are shown in Table 1. The following validation statistics were cal-

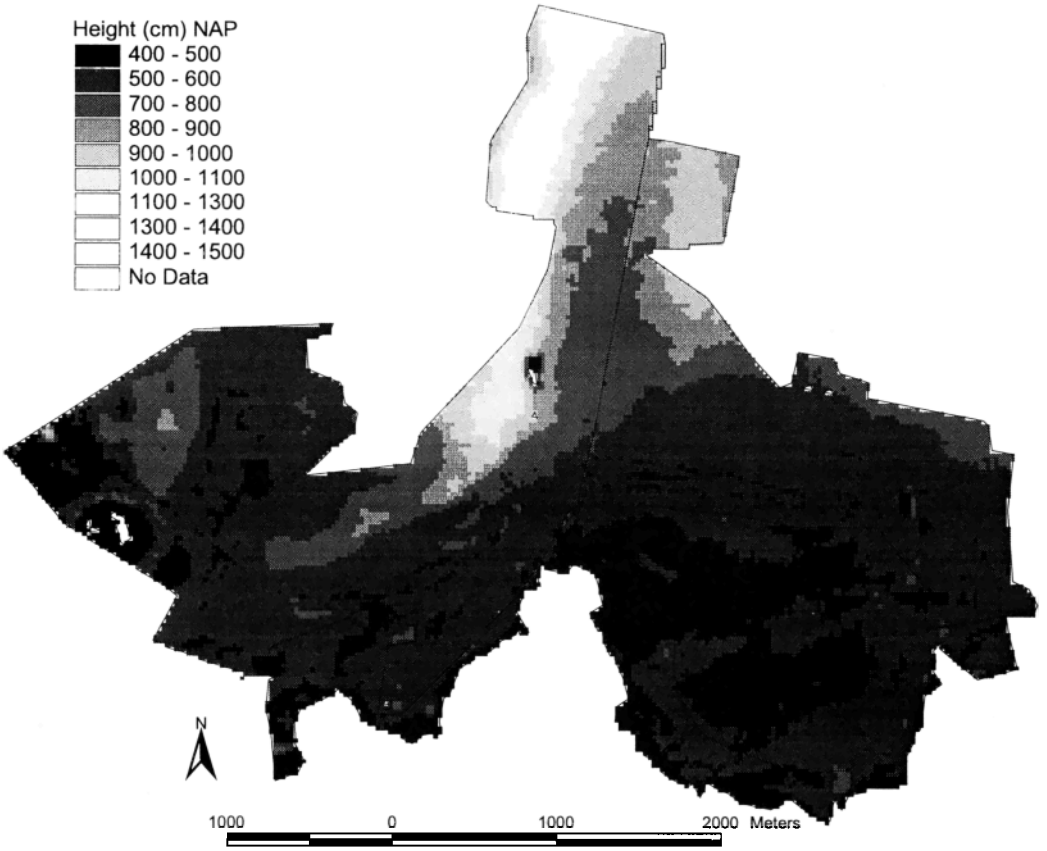

Figure 2. Map of surface elevations from the digital elevation model, 25 × 25 m resolution, and elevations derived from airborne laser scanning. NAP is Dutch ordnance level.

culated: the mean error (ME), a measure for bias or systematic error, the root-mean-square error (RMSE), a measure for accuracy or total error, and the mean absolute error (MAE), also a measure for accuracy but less sensitive to outliers. Table 1 shows that the OK, SK, and SKVk methods have little bias but are less accurate, whereas the KEDd and CM methods show notable bias but are more accurate. So the KEDd and CM methods show a larger systematic error and a smaller random error than the OK, SK, and SKVk methods. The cause of the systematic error of KEDd and CM probably lies in the extrapolation involved. Most time series locations are positioned in the areas with lower surface elevations. The relation between surface elevation and water table depth used in the external drift kriging approach is probably not representative for the higher areas, thus leading to an overestimation of the water table depth. Comparison of CM with KEDd shows little improvement. The reason is that the RMSE is largely determined by the quality of the estimate of the average water table depth, that is, the c parameter, which in both methods is estimated with external drift kriging. Finally, the SKVu method shows both large bias and low accuracy. Also, for this last method it was difficult to find a minimum value for (14), indicating that the number of parameters to be calibrated (25) was too large for the number of observations used.

Table 1. Validation Statistics of the Space-Time Kalman Filtering of the RARX Model for Different Methods of Regionalizing the ARX Parameters[a]

Type of Regionalization	ME, cm	RMSE, cm	MAE, cm
OK	5.8	39.4	38.7
SK	4.3	38.3	37.6
SKVk	0.3	35.3	34.4
SKVu	17.2	43.3	42.3
KEDd	21.4	31.7	30.3
CM	21.3	31.5	30.0
KEDs	10.9	13.8	12.4

[a]Abbreviations are as follows: ARX, auto autoregressive exogenous time series model; RARX, regionalized ARX; OK, ordinary kriging; SK, simple kriging; SKVk, simple kriging with known varying means; SKVu, simple kriging with unknown varying means; KEDd, kriging with surface elevations from the digital elevation map as external drift variable; CM, combination method a(SKVk), b(SKVk), c(KEDd), and σ(OK); KEDs, kriging with surface elevations from surveying as external drift variable (used as reference); ME, mean error; RMSE, root-mean-square error; and MAE, mean absolute error.

If KEDd is compared with KEDs, it shows that the quality of the auxiliary information is crucial. The accuracy reached with the surveyed surface elevations is very high. In fact, it is comparable with the accuracy reached for a single ARX model calibrated at a time series location. The RMSE calculated for the differences between the surveyed surface elevations and the DEM surface elevations is 20 cm. This shows that there is much room for improvement of the DEM and through the DEM the predictions with the RARX model. As an example, Figure 3 shows for two validation locations (see Figure 1) and the CM method the Kalman filter measurement updates and the associated 95% prediction interval together with the observations. To show the range of model performance, we pro-

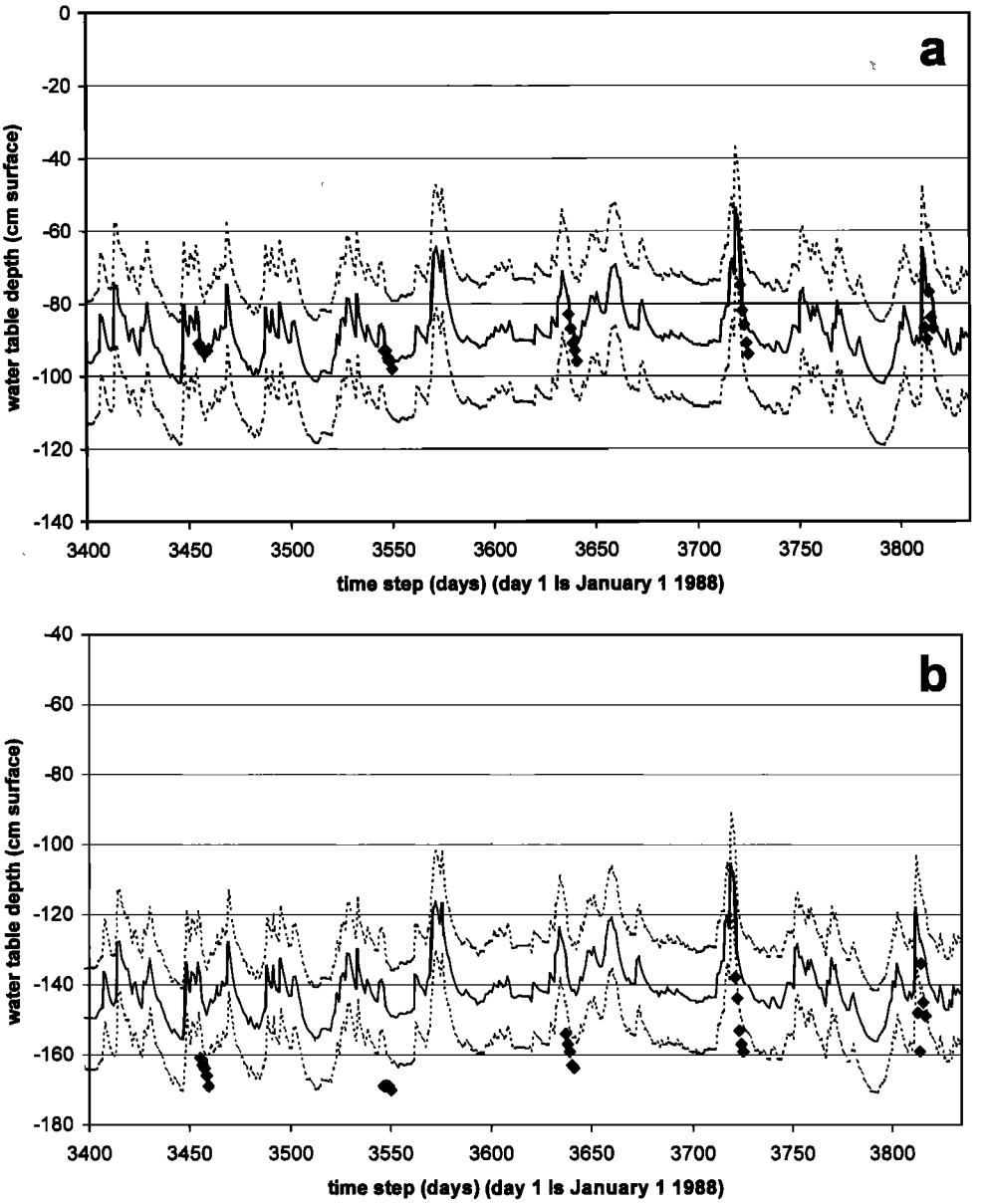

Figure 3. Example of measurement updates of water table depth (solid line), 95% prediction interval (dashed lines), and observations (diamonds) at two different validation locations: (a) one with excellent results and (b) one with poor results. For locations, see Figure 1.

vide a location with excellent results (Figure 3a) and a location with poor results (Figure 3b). Figure 3b shows that the poor fit mainly results from a systematic error. This was also true for other validation locations that performed poorly. These systematic errors are most likely caused by errors in the DEM, as can be seen when comparing methods KEDd and KEDs in Table 1. In sections 6.3–6.5 all calculations have been performed with the CM regionalization method.

We also investigated the effect of reducing the number of observations in time and space for the combination method. First, the CM method was applied using the first 13 and the subsequent 12 observations (of 25) at each calibration location (CMt). Second, 5 out of the 10 calibration locations were removed (CMs). The results are given in Table 2, which shows that reducing the temporal coverage of the observations has some effect, while no effect is observed when the spatial coverage is reduced. Obviously, this is not a general result. The ratio of these effects depends on the reaction time of the RARX model (the $a(\mathbf{x})$ parameters) compared to the spatial correlation of the noise process (the I parameter, about 200 m here).

Table 2. Effect of Reducing the Number of Observations in Time (CMt) and Space (CMs) When Compared to Using All Observations (CM) for the Combination Method

Method	ME, cm	RMSE, cm	MAE, cm
CM	21.3	31.5	30.0
CMt	23.4	35.3	34.4
CMs	22.8	31.0	28.7

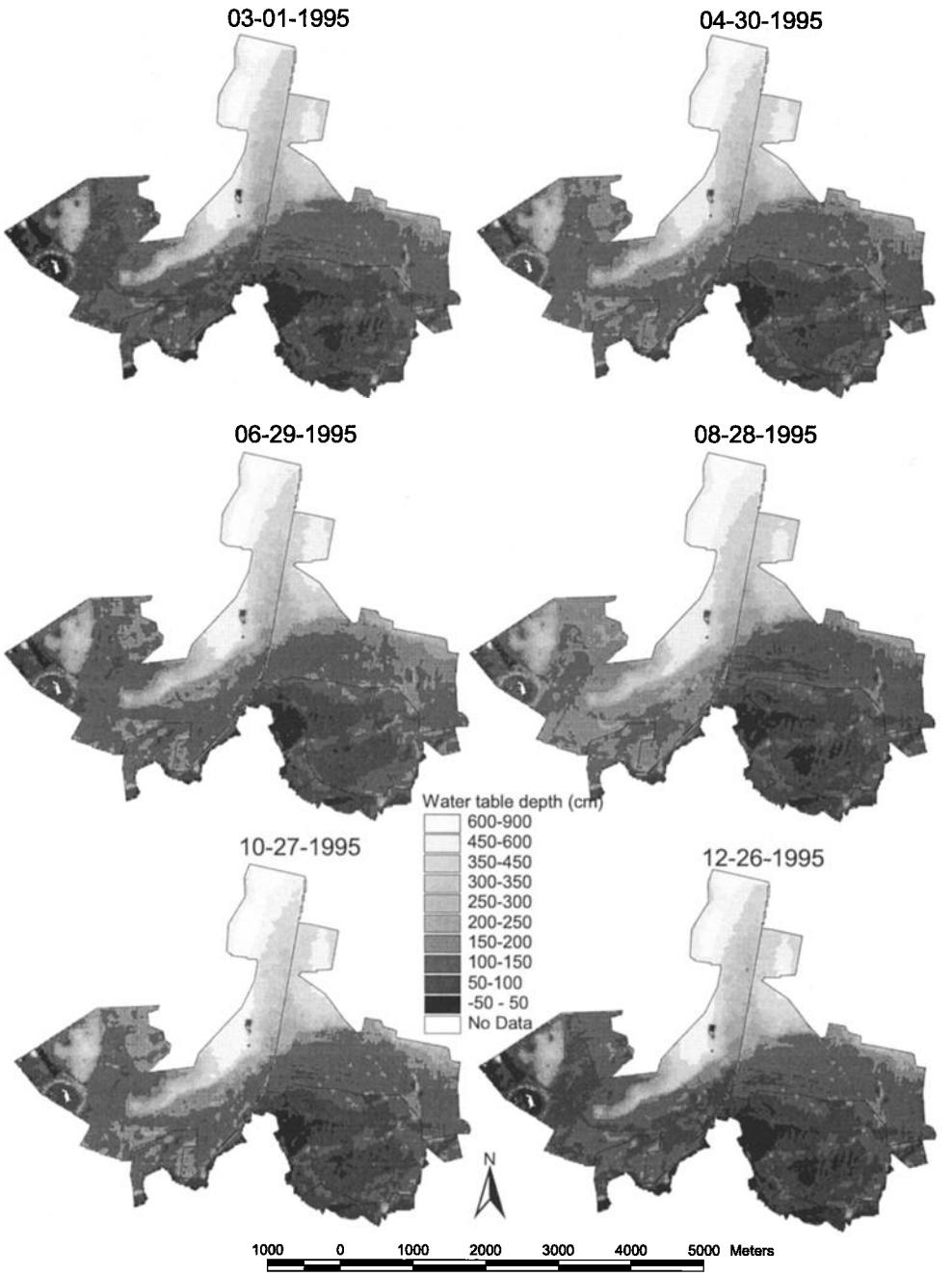

Figure 4. Six snapshots of the space-time predicted water table depth (measurement updates) covering the year 1995. Read 12-26-1995 as December 26, 1995.

6.3. Space-Time Prediction

The state is extended to include next to the time series locations and the calibration locations also the center locations of the 25 × 25 m resolution DEM of the area. This brings the total state to $N = 21{,}568$ locations. The Kalman filter was run for $K = 3834$ time steps, covering the period January 1, 1988, to June 30, 1998, which includes the period for which observations at the time series locations and the calibration locations were available. Figure 4 shows six snapshots of the space-time predicted water table depths covering the year 1995. Figure 5 shows a time series of predicted water table depth at one of the calibration locations (see Figure 1). This location is chosen because it shows nicely the effect of the updating. To further emphasize the updating effect, we also included a time series of water table depth that was only updated with the first half of the observations. Clearly, the high peak at the end of the period is not only caused by the precipitation surplus, such that the RARX model is not able to follow this variation. If observations are available, the Kalman filter will correct for this model inadequacy.

The space-time prediction method also yields prediction variances (i.e., the diagonal of the covariance matrix of the error in the measurement update: $\mathbf{\Sigma}_{t|t} = E\{[\hat{\mathbf{h}}_t(\mathbf{x}) - \mathbf{h}_t][\hat{\mathbf{h}}_t(\mathbf{x}) - \mathbf{h}_t]^T\}$). In Figure 6 a map is shown of the standard deviation of the error of the measurement update as calculated with the Kalman filter for December 15, 1997. Clearly, the

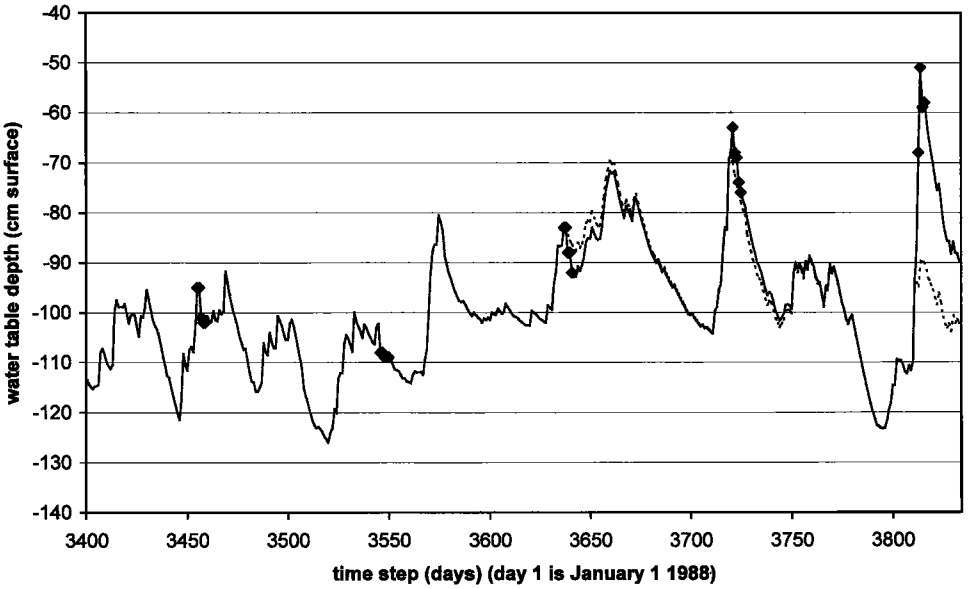

Figure 5. Time series of measurement updates of water table depth at a calibration location. Dashed line is only updated using the first half of the observations. For location, see Figure 1.

effect of the stratification that was used in regionalizing the $a(\mathbf{x})$ and $b(\mathbf{x})$ parameters is visible, while the influence of the observations is also visible. Close to the observations locations that have been recently observed, small prediction variances are calculated. The sudden jump across the catchment boundaries in the north of the study area is not that unrealistic. On the west side of this boundary, boulder clay is found at shallow depths. Both the textural content and the occurrence of the boulder clay is unknown, which means that we are very uncertain about the real water table depths in that area. Figure 7

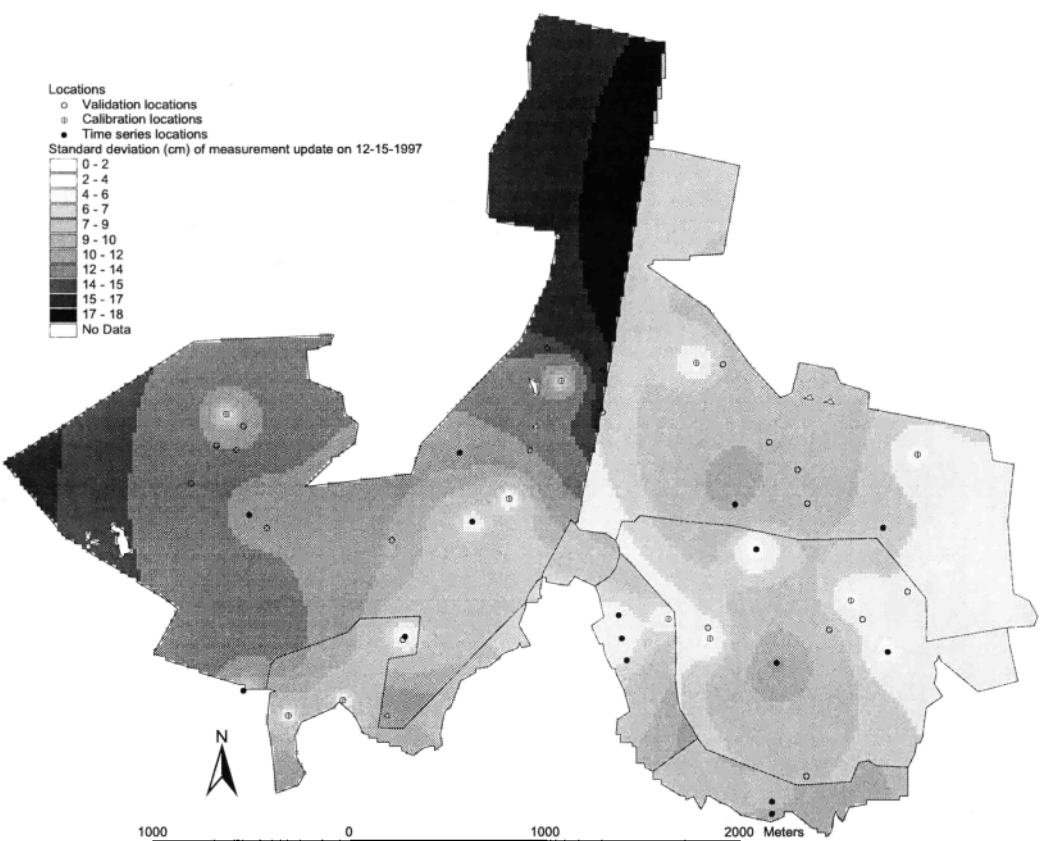

Figure 6. Map of the standard deviation of the error of the measurement update $H_t - \hat{H}_t$ calculated with the Kalman filter for December 15, 1997.

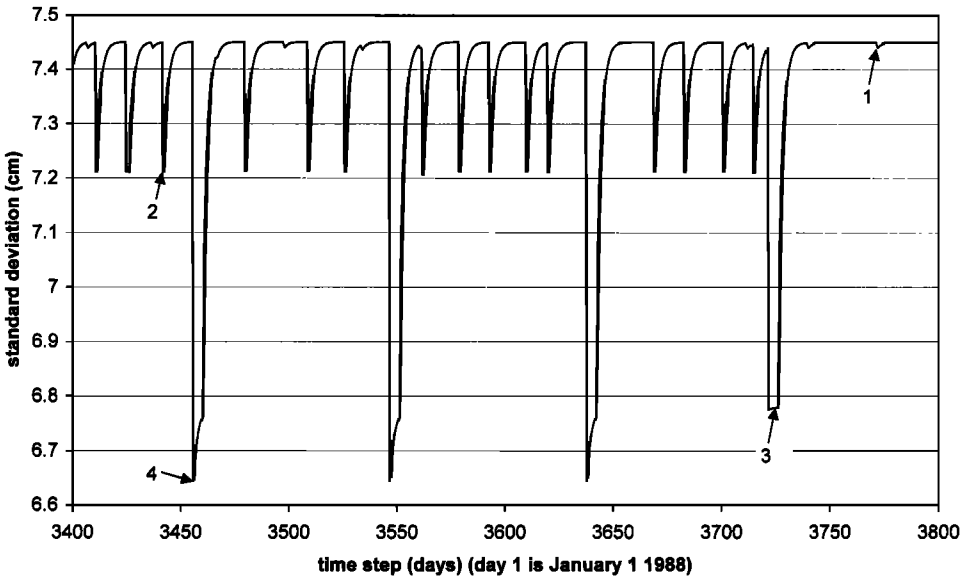

Figure 7. Example of the evolution of the standard deviation of the measurement update in time showing the influence of multiple nearby observations. For location, see Figure 1.

gives an example of the time evolution of the standard deviation of the measurement update error for a location where no observations are made (the same location as Figure 3b, see Figure 1). We can see the influence of at least three observation locations: (1) a time series location that is far away, leading to a very small dip of uncertainty (arrow 1); (2) a time series location that is closer, leading to a larger reduction of uncertainty (see arrow 2); (3) a calibration location with five observations in a row that is even closer, resulting in the largest uncertainty reduction (arrow 3). Arrow 4 denotes a time step at which observation types 2 and 3 are observed simultaneously.

The Kalman filter calculates these standard deviations based on the assumption of $\mathbf{h}_t$ being multi-Gaussian. Although this is a strong assumption, the advantage is that it can be used for network optimization, i.e., the optimal allocation of observations in both space and time, without the need to know the actual values at the projected observations.

6.4. Space-Time Conditional Simulation

As mentioned in section 5, certain applications require simulated realizations of the spatiotemporal stochastic process $\{H_t(\mathbf{x}), t = 0, 1, \ldots, K\}$ (taking both spatial and temporal dependence into account), where these realizations should be conditional to the observations. Using the method described in section 5, we used the Kalman filter with the reduced state approximation (see Appendix A, using a reduced state of 5% of the locations to approximate the Kalman gain) to simulate one conditional realization of $\{H_t(\mathbf{x}), t = 0, 1, \ldots, K\}$, with $t = 0$ on January 1, 1994, and $t = K$ on June 30, 1998. Figure 8 (right) shows one time slice on December 26, 1995. Comparison with the predicted water table depth on that date (left) shows little difference. The same was true for other realizations. Clearly, the uncertainty about the water table depth on that date was small compared to the variation in space.

6.5. Predicting Discharge From a Catchment With Surface Water Control

Knotters and Bierkens [2000] provided a physical interpretation of the ARX model based on the water balance of a soil column. From their analysis it follows that if the RARX parameters are known and the drainage base of the shallow groundwater is formed by the nearby surface waters, the specific discharge to these surface waters for a location $\mathbf{x}$ can be predicted as follows:

$$\hat{D}_t(\mathbf{x}) = \frac{1 - \hat{a}(\mathbf{x})}{\hat{b}(\mathbf{x})} [\hat{H}_t(\mathbf{x}) - \langle h_s \rangle], \tag{16}$$

where $\hat{D}_t(\mathbf{x})$ is the predicted specific discharge at location $\mathbf{x}$ and $\langle h_s \rangle$ is the average water level of the nearby surface waters. We stress that relation (16) is only valid if the surface water levels in the catchment can be set independently of the water table depth, for example, through pumps or adjustable weirs.

If almost all of the total discharge from the catchment is caused by drainage discharge from groundwater (no surface runoff), the catchment's discharge may be estimated by the average of the specific discharge (16) of all locations within the catchment. We attempted this for the catchment called Paardelanden (catchment number 3 in Figure 1). The average surface water levels for this small catchment were provided from the local water authority, who also provided the monthly averaged discharge from Paardelanden. Water levels in Paardelanden are maintained by pumping engines that are activated when surface water levels deviate too much from a target surface water level. From the pumping hours and pumping capacity an estimate of the monthly averaged discharge (mm d^{-1}) can be made.

Figure 9 denotes the measured monthly averaged discharge from Paardelanden together with the predicted monthly discharge. The predicted monthly discharge is obtained as follows. First, the daily discharges are estimated by averaging for each day the specific discharges at the locations within Paardelanden predicted with the space-time Kalman filter and (16). Next, for each month the daily discharges are averaged. Figure 9 shows that the predicted discharges overestimate the actual discharges during the growing season (April–September). However, if we would take into account that surface water levels during the growing season are kept at a higher level than average (this is done to achieve subsurface irrigation), predic-

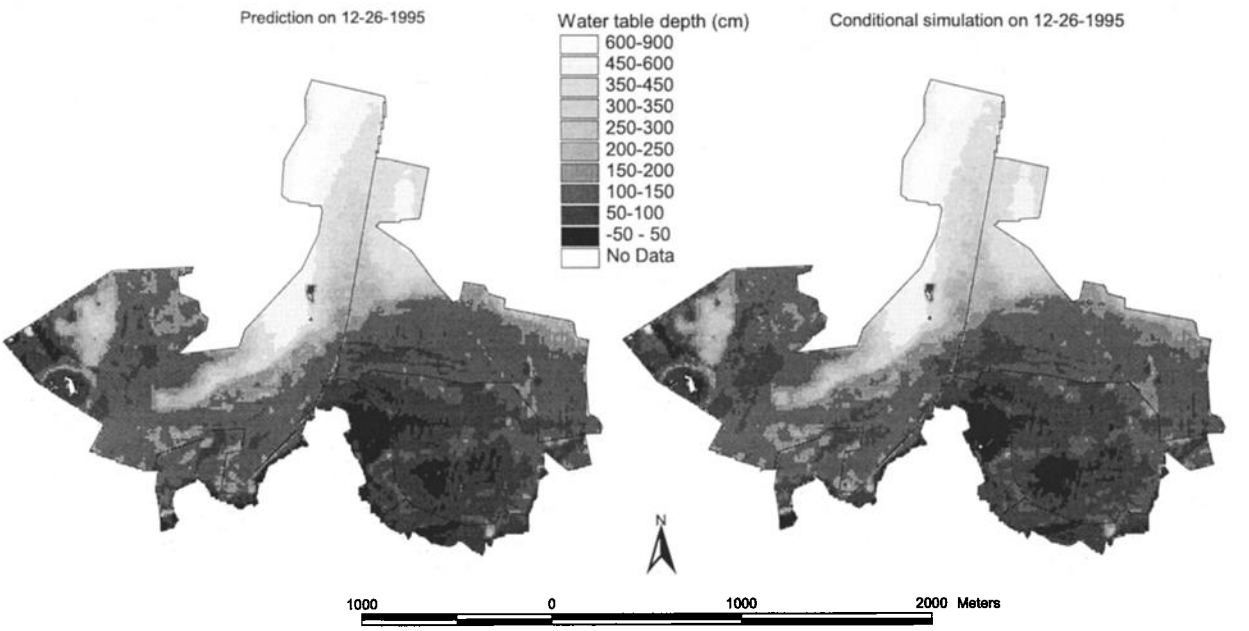

Figure 8. Time slice of a realization of (right) the conditionally simulated water table depth on December 26, 1995, as compared with (left) the predicted water table depth on that date.

tions for this period would probably be better. Moreover, Figure 9 also shows that, except for February 1997, the RARX model is able to predict the dynamical behavior of the monthly discharges reasonably well, particularly because the model was not calibrated to reproduce discharges. A possible explanation for the anomaly in February 1997 is that no excess water was pumped out of the catchment during that time, possibly to raise the surface water levels for the coming growing season.

If the February 1997 discharge is left out, the correlation coefficient between predicted and observed monthly discharge is 0.92. Although we realize that for daily discharges this correlation would be smaller, these results do suggest that a simple two-parameter (linear) relation is possible between observed and predicted discharge and therefore between observed discharge and predicted water table depth (through (16)). Such a relationship could be included in the observation equation (11) to improve the predictions of the water table depth if observations of discharge are present.

7. Conclusions and Discussion

A statistical method was developed for spatiotemporal modeling of water table depth. The method is based on the spatial application of an ARX model with precipitation surplus as the

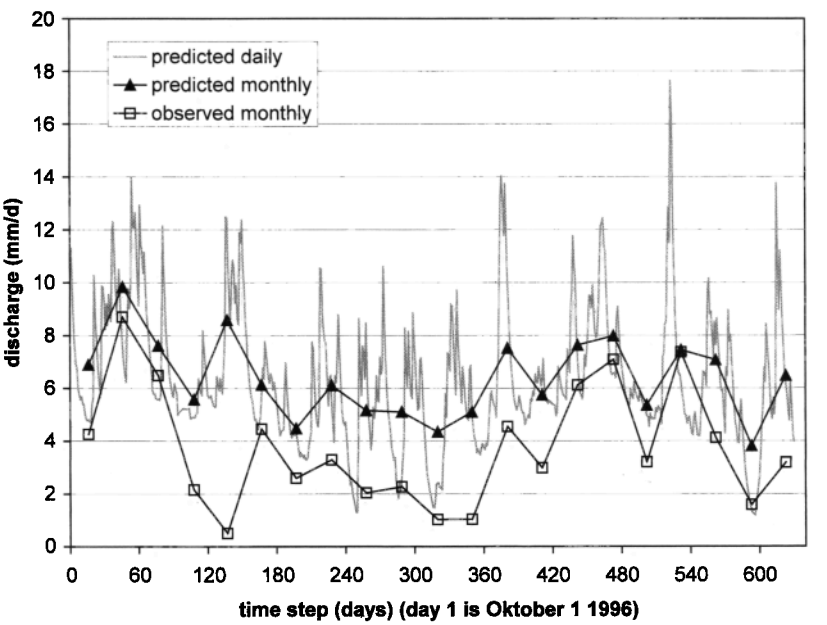

Figure 9. Predicted daily and monthly discharges and observed monthly discharges for the catchment Paardelanden (catchment 3 in Figure 1).

exogenous variable. The parameters of the ARX models are regionalized, i.e., spatially interpolated, using geostatistical methods and spatially exhaustive auxiliary information. The resulting regionalized ARX model or RARX model is embedded in a space-time Kalman filter to estimate the necessary semivariogram parameters used in the geostatistical interpolation. Together with the space-time Kalman filter the RARX model can be used for space-time prediction, network optimization in space and time, and space-time conditional simulation. Although the method was developed for modeling water table depth, its principles are more generally applicable, for instance, for the spatiotemporal modeling of soil moisture, surface temperature, and air pollution.

In a validation study involving the space-time prediction of water table depth, satisfactory results were obtained (RMSE 30 cm). It was also shown that the accuracy of the spatial auxiliary information, in our case the DEM, is a very important factor: using higher-quality elevation data as auxiliary information reduced the RMSE to 14 cm.

In the context of predicting water table depth a number of improvements could be made. First of all, the regionalization of the standard deviation of the system noise $\sigma(\mathbf{x})$ does not take account of the interpolation error made in the interpolation of the other RARX parameters, i.e., $a(\mathbf{x})$, $b(\mathbf{x})$, and $c(\mathbf{x})$. This could, for instance, be achieved by making the magnitude of $\hat{\sigma}(\mathbf{x})$ dependent on the kriging variance. The second improvement was already proposed in section 6.3, i.e., the improving the predictions of water table depth with discharge observations. A third improvement would be allowing the surface water levels to vary with time, which means that the c parameter becomes time dependent: $c(\mathbf{x}) \rightarrow c_t(\mathbf{x})$. Finally, the space-time Kalman filter can be used for on-line forecasting, using, for instance, weather forecasts. In combination with the possibility of analyzing the effects of varying surface water levels, the method would not only be suitable for inventory and monitoring but also for optimal control of the surface water network.

Appendix A: Storage Problems and Computation Times

A drawback of the space-time Kalman filter is its computational burden. If the number of state locations N is large, it becomes impossible to store the matrices $\mathbf{\Sigma}_{t|t-1}$ and $\mathbf{\Sigma}_{t|t}$, which are the covariance matrices of the error in the time update and measurement update, respectively. For instance, a seemingly small problem of 100×100 nodes already requires the storage of covariance matrices with 10^8 elements. Moreover, the computation time required to evaluate some of the matrix multiplications becomes excessive.

A1. Computational Problems

In the RARX model formulation, computational problems are not encountered. The reason lies in the structure of the system matrix $\mathbf{A}$. Because the RARX model is a collection of parallel 1-D models that have no lateral interaction, $\mathbf{A}$ is a diagonal matrix. Consequently, the number of matrix computations needed to run the Kalman filter evaluate is a factor N^2 smaller than for a full matrix $\mathbf{A}$.

A2. Storage Problems at Calibration

It can be shown that for diagonal $\mathbf{A}$, the vector $\mathbf{n}_t$ and the covariance matrix $\mathbf{Z}_t$ in (14) only depend on the state variables at those locations where in any of the time steps an observation is taken. This means that during the calibration of the RARX model it is permitted to use a state vector containing only the locations with observations (i.e., the locations with time series and the calibration locations with occasional observations). In most practical problems these numbers are limited, so that no storage problems will occur during calibration.

A3. Storage Problems at Space-Time Prediction

If the Kalman filter is used for space-time prediction of the complete state, usually the full covariance matrices must be stored. For a practical problem such as presented in the case study, this would lead to storage problems. However, because $\mathbf{A}$ is diagonal, the optimal predictions $\hat{H}_t(\mathbf{x})$ and the associated error variance $E\{[H_t(\mathbf{x}) - \hat{H}_t(\mathbf{x})]^2\}$ at each location can be obtained independently of those at other locations. So if the prediction and the prediction variance are the only properties of interest, i.e., not the full covariance matrices $\mathbf{\Sigma}_{t|t-1}$ and $\mathbf{\Sigma}_{t|t}$, the predictions can be obtained location by location. So similar to kriging, for each (nonobserved) location the Kalman filter is run separately, using a state vector containing all the locations with observations (time series locations and calibration locations) and the one location where the optimal predictions are required. This way, only small covariance matrices have to be stored.

A4. Storage Problems at Conditional Space-Time Simulation

If realizations of $\{H_t(\mathbf{x}), t = 0, 1, \ldots, K\}$ are simulated which are conditional to the observations, in theory the location by location method could be used also. However, this would require the storage of $K + 1$ (one for every time step) simulated noise fields of size N to be able to enter the right noise time series at each location. The storage requirements would be enormous. However, simulation of the full state would require the storage of the full covariance matrices $\mathbf{\Sigma}_{t|t-1}$ and $\mathbf{\Sigma}_{t|t}$ to be able to calculate the correct Kalman gain $\mathbf{K}_t$ (the Kalman gain is used to calculate the measurement update $\hat{\mathbf{h}}_t$ from weighting the observations $\mathbf{y}_t$ and the time update $\bar{\mathbf{h}}_t$). Again, this would lead to serious storage problems. To circumvent the last problem, we applied a "reduced state approximation" as follows: (1) From all the state locations a smaller subset is selected (e.g., a coarser grid) that has a similar spatial extent as the total state. (2) The Kalman filter is run as follows: The time update $\bar{\mathbf{h}}_t$ is calculated for the full state (with (15)). The covariance matrices $\mathbf{\Sigma}_{t|t-1}$ and $\mathbf{\Sigma}_{t|t}$ are calculated for the reduced state. From these the Kalman gain $\mathbf{K}_{r,t}$ is calculated for the reduced state. The Kalman gain for the full state is approximated by interpolating from the reduced state locations to the full state locations using inverse squared distance: $\mathbf{K}_{r,t} \rightarrow \hat{\mathbf{K}}_t$. Value $\hat{\mathbf{h}}_t$ is calculated for the full state using the approximated Kalman gain $\hat{\mathbf{K}}_t$.

Acknowledgments. This research benefited greatly from discussions with A. W. Heemink (Faculty of Information Technology and Systems, Delft University of Technology), C. B. M. te Stroet (Netherlands Institute for Applied Geoscience TNO), and P. A. Troch (Sub-Department of Water Resources, Wageningen University). The comments of associate editor S. E. Silliman (Department of Civil Engineering and Geological Sciences, University of Notre Dame) and of an anonymous reviewer significantly improved the paper. This research was funded (SEO-I) by The Netherlands Ministry of Agriculture, Nature Management and Fisheries.

References

Angulo, J. M., W. González-Manteiga, M. Ferrero-Bande, and F. J. Alonso, Semi-parametric statistical approaches for space-time process prediction, *Environ. Ecol. Stat.*, *5*, 297–316, 1998.

Bennet, R. J., *Spatial Time Series: Analysis-Forecasting-Control*, Pion, London, 1979.

Bierkens, M. F. P., M. Knotters, and F. C. van Geer, Calibration of transfer function-noise models to sparsely or irregularly observed time series, *Water Resour. Res.*, *35*(6), 1741–1750, 1999.

Bogaert, P., Comparison of kriging techniques in a space-time context, *Math. Geol.*, *28*(1), 73–86, 1996.

De Bruin, H. A. R., The determination of (reference crop) evapotranspiration from routine weather data, in *Comissie Hydrologisch Onderzoek TNO, Vers Meded.*, *28*, pp. 25–37, The Hague, Netherlands, 1981.

Evensen, G., and P. J. van Leeuwen, Advanced data assimilation based on ensemble statistics, in *Second International Symposium on Assimilation of Observations in Meteorology and Oceanography*, Tokyo, pp. 153–158, World Meteorol. Organ., Geneva, 1995.

Goovaerts, P., *Geostatistics for Natural Resources Evaluation*, Oxford Univ. Press, New York, 1997.

Guenni, L., M. F. Hutchinson, W. Hogarth, C. W. Rose, and R. Braddock, A model for seasonal variation of rainfall at Aidelade and Turen, *Ecol. Model.*, *85*, 203–217, 1996.

Guttorp, P., W. Meiring, and P. D. Sampson, A space-time analysis of ground-level ozone data, *Environmetrics*, *5*, 241–254, 1994.

Haslett, J., and A. E. Raftery, Space-time modeling with long-memory dependence: Assessing Ireland's wind power resource (with discussion), *Appl. Stat.*, *38*(1), 1–50, 1989.

Heuvelink, G. B. M., P. Musters, and E. J. Pebesma, Spatio-temporal kriging of soil water content, in *Geostatistics Wollongong '96*, vol. 2, edited by E. Baaffi and N. Schofield, pp. 1020–1030, Kluwer Acad., Norwell, Mass., 1997.

Hipel, K. W., and A. I. McLeod, *Time Series Modelling of Water Resources and Environmental Systems*, Elsevier Sci., New York, 1994.

Huang, H., and N. Cressie, Spatio-temporal prediction of snow water equivalent using the Kalman filter, *Comput. Stat. Data Anal.*, *22*, 159–175, 1996.

Hutchinson, M. F., Stochastic space-time weather models from ground-based data, *Agric. For. Meteorol.*, *73*, 237–264, 1995.

Knotters, M., and M. F. P. Bierkens, Physical basis of time series for water table depths, *Water Resour. Res.*, *36*(1), 181–188, 2000.

Knotters, M., and M. F. P. Bierkens, Predicting water table depths in space and time using a regionalised time series model, *Geoderma*, in press, 2001.

Kyriakidis, P. C., and A. G. Journel, Geostatistical space-time models: A review, *Math. Geol.*, *31*(6), 651–684, 1999.

Pfeifer, P. E., and S. J. Deutsch, A three-stage iterative procedure for space-time modeling, *Technometrics*, *22*, 35–47, 1980.

Press, W. H., B. P. Flannery, S. A. Teukolsky, and W. T. Vetterling, *Numerical Recipes: The Art of Scientific Computing*, Cambridge Univ. Press, New York, 1986.

Rouhani, S., and T. J. Hall, Space-time kriging of groundwater head data, in *Geostatistics*, vol. 2, edited by M. Armstrong, pp. 639–650, Kluwer Acad., Norwell, Mass., 1989.

Schweppe, F. C., *Uncertain Dynamic Systems*, Prentice-Hall, Englewood Cliffs, N. J., 1973.

Van Geer, F. C., and A. F. Zuur, An extension of Box-Jenkins transfer/noise models for spatial interpolation of groundwater head series, *J. Hydrol.*, *192*, 65–80, 1997.

Van Geer, F. C., C. B. M. te Stroet, and Z. Yangxiao, Using Kalman filtering to improve and quantify the uncertainty of numerical groundwater simulations, 1, The role of system noise and its calibration, *Water Resour. Res.*, *27*(8), 1987–1994, 1991.

Wikle, C. K., and N. Cressie, A dimension-reduced approach to space-time Kalman filtering, *Biometrika*, *86*(4), 815–829, 1999.

Winter, T. C., D. O. Rosenberry, and A. M. Sturrock, Evaluation of 11 equations for determining evaporation for a small lake in the north central United States, *Water Resour. Res.*, *31*(4), 983–993, 1995.

M. F. P. Bierkens, M. Knotters, and T. Hoogland, Alterra, Wageningen University and Research Centre, P.O. Box 47, 6700 AA Wageningen, Netherlands. (M.F.P.Bierkens@Alterra.wag-ur.nl)

(Received February 2, 2000; revised October 30, 2000; accepted October 30, 2000.)